International Research Journal of Engineering and Technology (IRJET) e-ISSN: 2395-0056
Volume: 05 Issue: 11 | Nov 2018 www.irjet.net p-ISSN: 2395-0072

Thermal and fluid flow analysis of a Heat Exchanger: "A Comprehensive report"

Nabhanshul Satra[1], Shantanu Dixit[2]

[1,2]B.E. Scholar, Dept. of Mechanical Engineering, BIT Durg, Chhattisgarh, India

---

Abstract - *Heat exchangers are the most common thermal systems which have conventionally been used in various environmental and industrial usages. This paper concentrates on comprehensive research report in the field of fluid flow and heat transfer in heat exchanger. To improve the thermal performance of heat exchanger various techniques have been used such as implementing various surface textures such as corrugated, wavy, dimpled, etc, flow along various channel such as sinusoidal, wavy, u shaped, etc. Using with different fluid with combination of Nano-particles. The main purpose of using these is to enhance the mass and heat transfer phenomenon, related with large pressure discrepancy. Essentially, the fully developed flow over an arbitrary surface, in any laminar or turbulent flow, is greatly advanced and complex than the flow over a smooth surface.*

Several types of research have been carried out experimentally, numerically and computationally to explore the flow characteristics over various types of heat exchanger for various engineering applications which have been stated in this paper.

Key Words: Heat transfer, Mass transfer, Reynolds Number, CFD.

1. INTRODUCTION

Heat exchanger (HX) is a heat transmission device that allows heat transfer between two fluids which are at different temperatures [1]. Heat transfer occurs from higher temperature fluid to lower temperature fluid. In most heat-related devices, heat transfer surface separates two fluids which may vary with different types of HXs. The classification of HX is based on their types of construction, flow arrangements, surface compactness, and transfer process, pass arrangement, phase of fluids, and heat transfer mechanism. Depending upon the flow arrangement, heat exchangers can be parallel flow, counter flow, cross flow, cross-counter flow, etc. In parallel flow heat exchanger, flow direction of both hot and cold fluid remains same while in counter flow heat exchanger, flow direction of both fluids is reversed which yields better heat transfer performance [2]. According to the pass arrangement classification of HX, the most common shell and tube HX can be one shell pass and two tube passes or two shell passes and four tube passes depending upon the industrial requirements. The construction and performance features of different types of heat exchanger [3–5] are documented in Fig 1. It is seen from fig that there are various type CHXs such as Shell and tube heat exchanger (STHXs), Plate and fin heat exchanger (PFHX), Spiral plate heat exchangers (SPHX), Plate and frame heat exchangers (PFHX), Printed circuit heat exchanger (PCHEs), Marbond Heat Exchanger, Continuous smooth fins and circular tube HX, wavy fins and circular tube HX, Continuous smooth fins and non-circular tube HX etc. Among these, shell and tube heat exchanger (STHXs) is widely used due to its flexibility and innovative design. But it requires larger area to be placed and great amount of space during removing baffles. PFHXs are preferred over extended surface HXs due to its highly effective thermal performance which handles multiple streams quite well. That's why PFHXs are used in compressor coolers, conditioning plant, and in others cryogenic application. While considering the applications in chemical industries, Fuel processing, Power and energy and refrigeration systems, PCHEs are widely used. PCHEs are made of Stacks of plates of Stainless steel and titanium material bonded together through diffusion in the pressure and temperature.

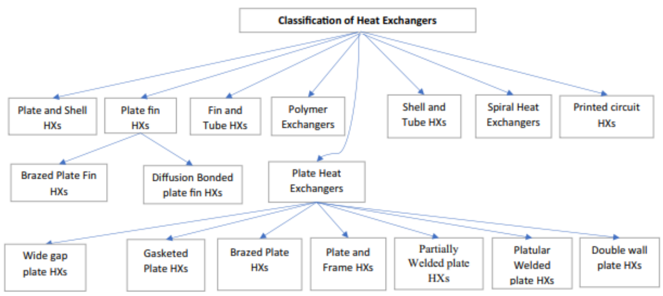

Fig. 1. Flow diagram demonstrating different types of heat exchangers.

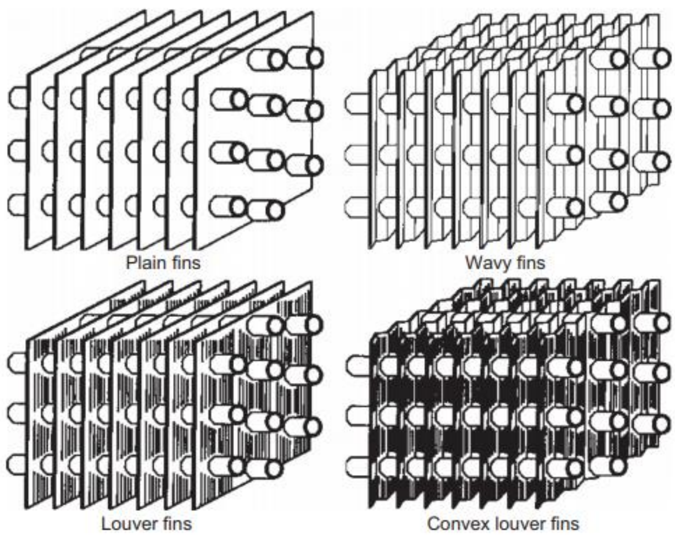

2. Schematic diagram of various fin patterns for fin-and-tube heat exchangers [6]

Since the creation of the Plate Heat Exchanger (PHE) in 1921 for utilization in the dairy technology, it has been extensively employed in different areas. PHE includes a set of thin plates and a frame to support them. The working fluid moves inside the gap between adjacent plates. The heat transfer surface can be simply modified with adding or removing plates, and the heat transfer rate can be adjusted. With intensifying requirements for energy savings, the PHEs now play a key role in industries. A PHE with great efficacy can considerably decrease energy waste. There are many kinds of PHEs, such as chevron, herringbone, and wash board. From these types, the chevron PHE is the most extensively utilized

2. Mathematical Modeling

For the fluid flow through pipe, duct and channel the conventional governing equations are the **Navier–Stokes equations** can be written in the most useful form for the development of the finite volume method:

$$\rho\frac{Du}{Dt} = -\frac{\partial p}{\partial x} + div(\mu\, grad u) + S_{Mx} \quad (1)$$

$$\rho\frac{Dv}{Dt} = -\frac{\partial p}{\partial y} + div(\mu\, grad v) + S_{My} \quad (2)$$

$$\rho\frac{Dw}{Dt} = -\frac{\partial p}{\partial z} + div(\mu\, grad w) + S_{Mz} \quad (3)$$

Governing equations of the flow of a compressible Newtonian fluid

Continuity

$$\frac{\partial \rho}{\partial x} + div(\rho u) = 0$$

x-momentum

$$\frac{\partial(\rho u)}{\partial x} + div(\rho u u) = -\frac{\partial p}{\partial x} + div(\mu\, grad u) + S_{Mx} \quad (4)$$

y-momentum

$$\frac{\partial(\rho v)}{\partial y} + div(\rho v u) = -\frac{\partial p}{\partial y} + div(\mu\, grad v) + S_{My} \quad (5)$$

z-momentum

$$\frac{\partial(\rho w)}{\partial z} + div(\rho w u) = -\frac{\partial p}{\partial z} + div(\mu\, grad w) + S_{Mz} \quad (6)$$

Energy

$$\frac{\partial(\rho i)}{\partial t} + div(\rho i u) = -p\, div u + div(k\, grad T) + \Phi + S_i \quad (7)$$

Using various correlation FEV results have been compared analytically

$$h_f = f\frac{LV^2}{D_h 2g}$$

Where,

f is the friction factor for fully developed laminar flow

L: length of the channel, duct, pipe

V: mean velocity of the flow

d: diameter of the pipe

f is the friction factor for fully developed laminar flow:

$$f = \frac{64}{Re} \text{ (For Re<2000) } \quad Re = \frac{\rho u_{avg} d}{\mu}$$

C_f is the skin friction coefficient or Fanning's friction factor.

For Hagen-Poiseuille flow: $C_f = \tau_{wall} l \frac{1}{2}\rho u_{avg}^2 = \frac{16}{Re}$

For turbulent flow: $\frac{1}{\sqrt{f}} = 1.74 - 2.0\log_{10}\left[\frac{\varepsilon_p}{R} + \frac{18.7}{Re\sqrt{f}}\right]$ Moody's Chart

R: radius of the channel, duct, pipe

ε_p: degree of roughness (for smooth channel, duct, pipe, $\varepsilon_{p=0}$)

$Re \rightarrow \infty$: Completely rough channel, duct, pipe.

3. Literature Review

Tiwari et al. [7] explored the heat transfer and pressure drop characteristics in a chevron-type corrugated PHE using CeO2/water nanofluid as the coolant. The experiments were aimed for determining the heat transfer and pressure drop performance at the wide range of concentrations (0.5–3 vol%) for various fluid flow rates (1–4 lpm), and operating temperatures. Optimum concentration for CeO2/water nanofluid was determined as well, which yielded maximum heat transfer improvement over base fluid. It was found that the nanofluid in the PHE has maximum of 39% higher heat transfer coefficient compared to water at optimum concentration of 0.75 vol%. Moreover, the heat transfer coefficient increased with an increase in the volume flow rate of the hot water and nanofluid and increased with a decrease in the nanofluid temperature.

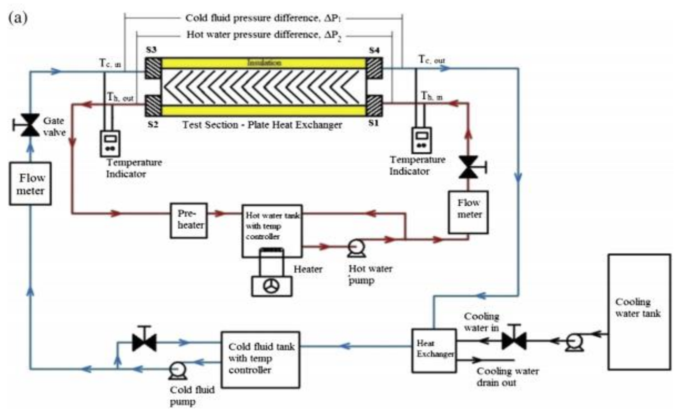

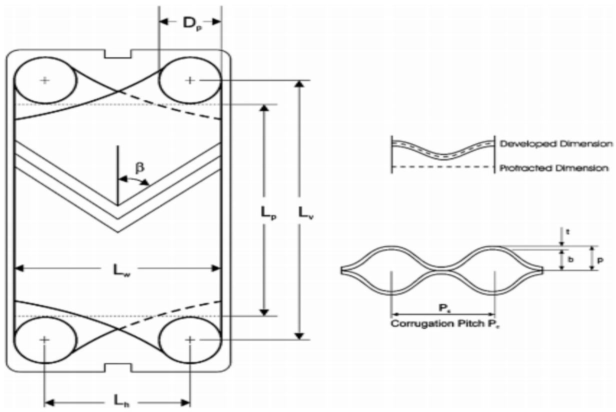

Fig 3 Experimental setup (a) schematic of the test facility (b) photograph of the test facility

Kabeel et al. [8] developed an experimental setup to study the PHE thermal characteristics including heat transfer coefficient, effectiveness, transmitted power and pressure drop at different volume fractions of Al2O3 nanomaterial in pure water. A pronounced increase in both heat transfer coefficient and transmitted power was observed by increasing the concentration. The maximum increase in heat transfer coefficient was reached 13% for a concentration of 4%. Moreover, both pressure drop and required pumping power increased with the increase in Reynolds number. The maximum increase in pressure drop was recorded 45% above the base fluid at concentration of 4%. The schematic of the chevron plate used and corrugation dimensions have been illustrated.

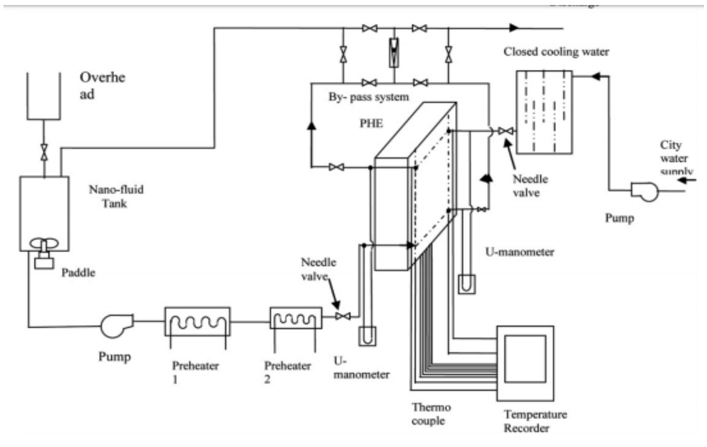

Fig 4 Experimental setup.

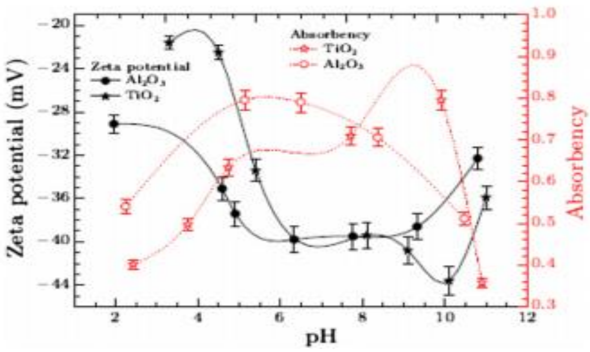

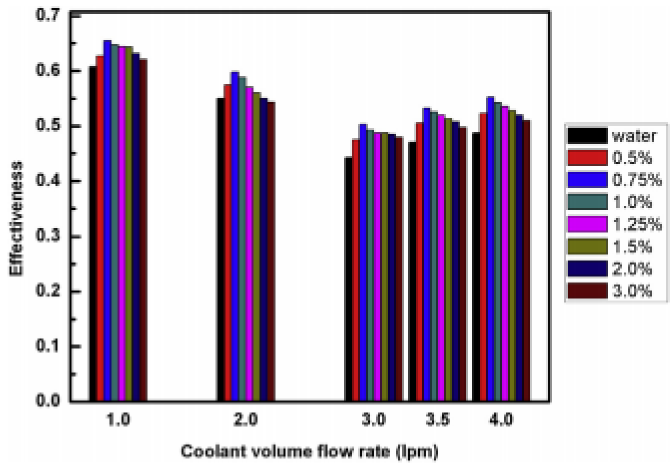

Fig. 5 The changes of zeta potential and absorbency for Al_2O_3e and TiO_2ewater nanofluids as a function of Ph value

In the experimental study of Wang in Ref. [9] of fin-tube heat exchanger with louver fins, the heat transfer and friction characteristics were presented. It was established that for multiple tube row number the effect of fin spacing on the convex louver fin configuration's heat transfer performance is higher at Fp = 2.54 mm as compared to Fp = 1.69 mm and Fp = 1.27 mm at low Reynolds number (Re) and reverse trend is exhibited in higher flow region. It was determined that at higher value of fin spacing the friction factor starts decreasing at Re < 2000. While fin spacing effect is not pronounced at higher Re number region. But the study conducted experimentally by Kim [10] concluded that effect of the fin pitch has no influence on the heat transfer performance and friction factor. It was noticed that louver fin heat exchangers have higher j and f factor as compared to the slit fin heat exchangers. The comparison was performed between the louver, slit and plain fin experimentally to observe the heat transfer and friction characteristics of these heat exchangers. It was found that the j factor of louver fin was 87% larger than that of the plain fin and the average f factor is 155% larger while for the slit fins the j factor was 84% larger than the plain fin, and the average f factor was 71% larger than the plain fin.

Jadavi et al. [11] study SiO2, TiO2 and Al2O3 are applied in a plate heat exchanger and the effects on thermo-physical properties and heat transfer characteristics are compared with the base fluid. Since it is desired to minimize the pressure drop, the influence of nanofluid application on pressure drop and entropy generation is investigated. It is concluded that the thermal conductivity, heat transfer coefficient and heat transfer rate of the fluid increase by adding the nanoparticles and TiO2 and Al2O3 result in higher thermo-physical properties in comparison with SiO2. The highest overall heat transfer coefficient was achieved by Al2O3 nanofluid, which was 308.69 W/m2 .K in 0.2% nanoparticle concentration. The related heat transfer rate was improved around 30% compared to SiO2 nanofluid. In terms of pressure drop, SiO2 shows the lowest pressure drop, and it was around 50% smaller than the pressure drop in case of using TiO2 and Al2O3.

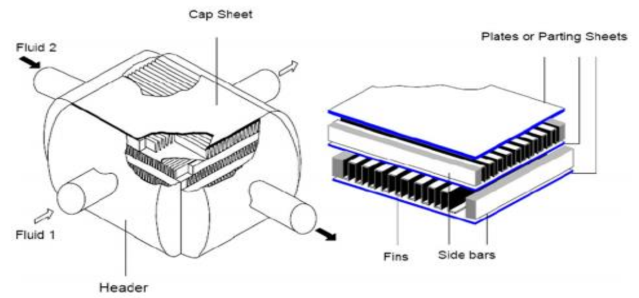

Fig. 6 Schematic of plate fin heat exchanger

Timo et al. [12] study the effect of using nanofluids in streams transferring heat from different processes by optimizing the total annual cost of a heat exchanger network. These costs include the cost of hot and cold utilities, heat exchanger investment costs and pumping costs. A modified version of the well-known Synheat superstructure is used as the optimization model in comparing the different fluids (water and five nanofluids) in two examples. Some key parameters (electricity price and annuity factor) are varied in these two examples. The results show that nanofluids can in some cases save total annual costs and especially if electricity prices are low compared to other factors. This is true especially for MgO1.0% which outperformed water and the other nanofluids in normal price conditions. But altogether it is evident that most, and in some cases all, of the benefits provided by nanofluids to improved heat transfer, is canceled out by the increased pressure drops.

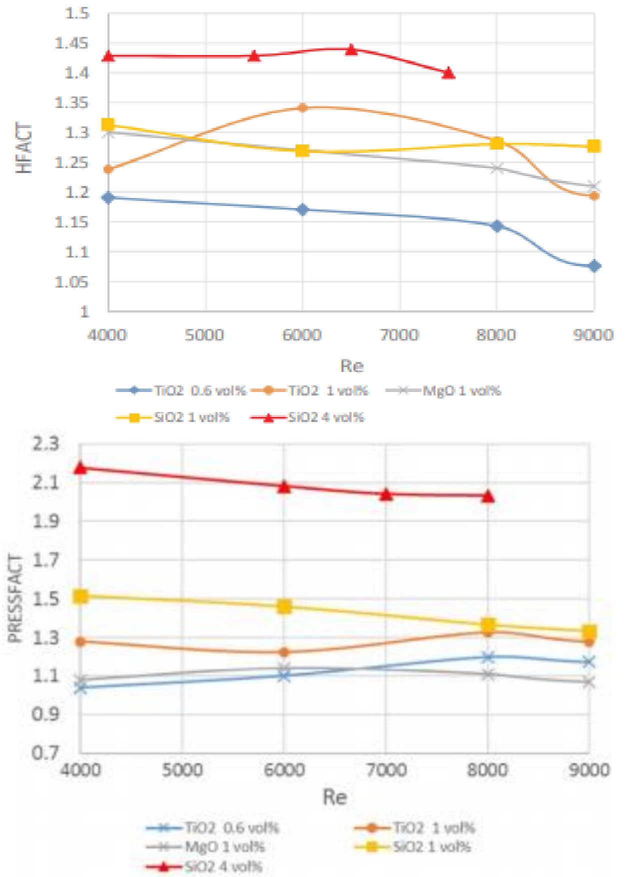

Fig. 7 HFACT as a function of the Reynolds number for different nanofluids and PRESSFACT as a function of the Reynolds number for different nanofluids.

Junyub et al. [13] study, the condensation heat transfer characteristics of R245fa in a shell and plate heat exchanger (SPHE) are measured and analyzed by varying the mean vapor quality from 0.16 to 0.86, mass flux from 16.0 to 45.0 kg m−2 s−1, heat flux from 1.3 to 9.0 kW m−2, and saturation temperature from 90 to 120 °C for high-temperature heat pumps (HTHPs). The condensation heat transfer coefficient and frictional pressure drop are shown to increase with increasing mean vapor quality and mass flux and with decreasing saturation temperature. The condensation heat transfer coefficient of R245fa in SPHE is on average 5.9% lower than that in the brazed plate heat exchanger (BPHE) with a similar effective heat transfer area. However, the average two-phase frictional pressure drop of R245fa in SPHE is 16.7% lower than that in BPHE. Empirical correlations for the condensation heat transfer coefficient and two-phase frictional pressure drop in SPHE are developed with mean absolute errors of 8.2% and 9.4%, respectively.

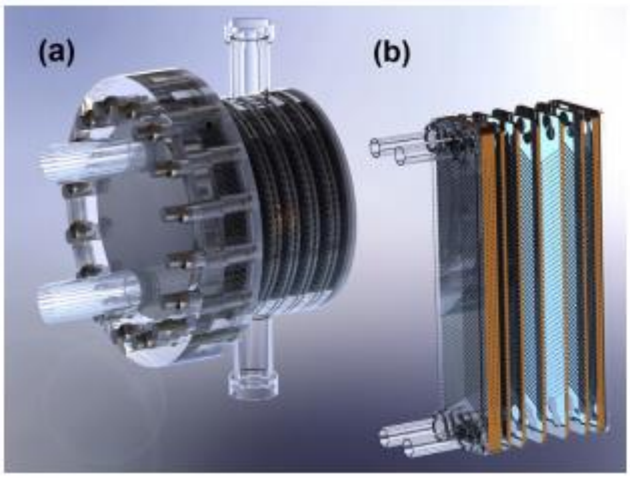

Fig. 8. (a) SPHE and (b) BPHE

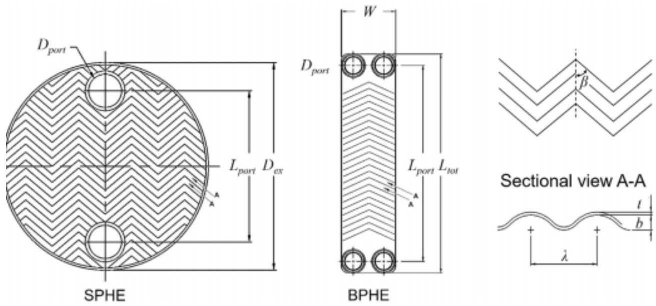

Fig. 9 Details of tested SPHE and BPHE.

Kafel et al. 2017 compares the performance of smooth, corrugated shell and corrugated tube exchanger. They also analyzed the distinct arrangements of concave and convex type of corrugated tubes. The exergy losses due to simultaneous employing of corrugated tubes as the inner and outer tube in heat exchanger have been reported. In their work experimental based parametric exergy analysis has been carried out. The result reveals that the corrugations lead to enhancement in both exergy loss and NTU. Moreover they also observed that heat exchanger made of convex corrugated tube and concave corrugated shell.

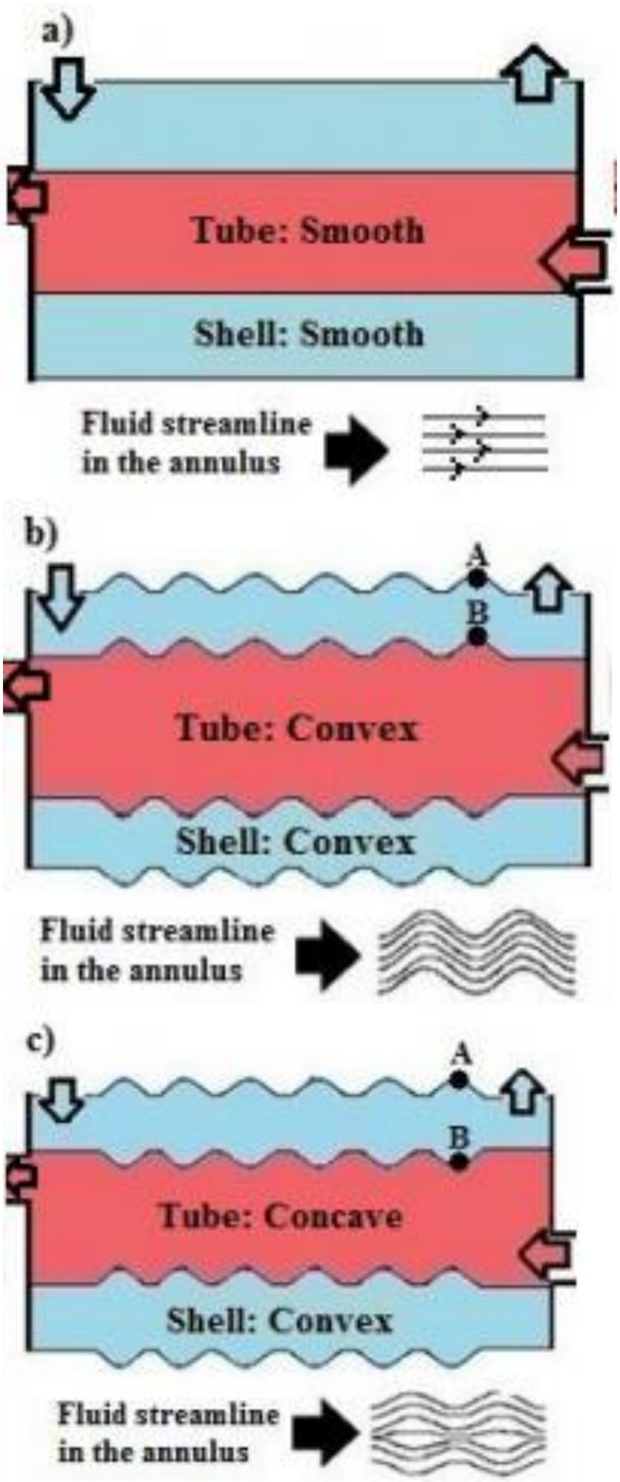

Figure 10The effect of arrangement type on annulus fluid streamline [14]

Wongwises [15] experimentally examined the influence of corrugation pitch on the condensation heat transfer and pressure drop of R-134 inside horizontal corrugated tube. Their results illustrates that the corrugated tube has heat transfer coefficient and pressure drop in comparison with smooth tube.

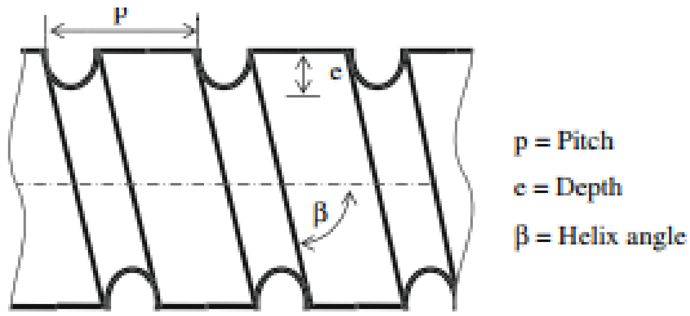

Figure 11 Drawing of a helically corrugated tube.

Aroonrat et al. [16] performed an experimental investigation on evaporation heat transfer and pressure drop of R-134 through a vertical corrugated tube. With having varying corrugation pitches. The heat transfer and pressure drop between smooth and corrugated tube have been compared and result shows that in corrugated tube have higher heat transfer coefficient and frictional pressure drop than smooth tube. They also concluded that as the corrugation pitch decreases, heat transfer coefficient and frictional pressure drop increases.

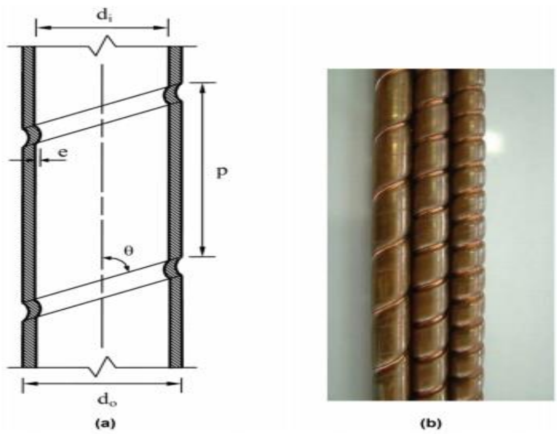

Figure 12 Corrugated tube: (a) sketch and (b) actual photograph. (color figure available online) [16]

Zhenping et al. 2017 examined the heat transfer and flow characteristics of half-corrugated microchannels. They compare the thermal performance and pressure drop between flat-bottom copper and half-corrugated microchannels. They found that the half-corrugated microchannels have superior thermal-hydraulic performance.

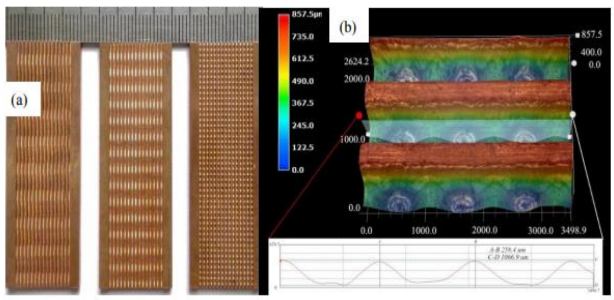

Figure 13 Morphologies of different microchannels: (a) appearance of half-corrugated microchannels with different wavelength;(b) surface profile of microchannel of MCH-31 [17]

Zhang and Che [5] numerically examined the thermal hydraulic performance of corrugation shape influence of corrugated plates. The governing equations and have been solved by using finite volume method and Lam-Bremhorst low Reynolds number turbulence model has been considered. A CFD analysis was carried out by using commercial software such as GAMBIT/FLUENT. It was observed that for sharp corrugations pressure drop and heat transfer coefficient was higher as compared to the smooth corrugations. They also conclude that the average Nusselt numbers and friction factor were about 1–4 times superior for the trapezoidal corrugated channel as compared to the elliptic corrugated channel.

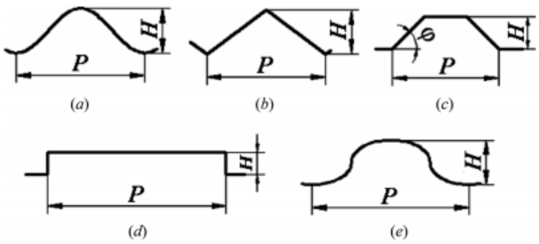

Figure 14 Corrugation profiles. (a) Sinusoidal curve, (b) triangular curve, (c) trapezoidal curve, (d) rectangular curve, and (e) elliptic curve. [18]

Islamoglu et al.2008 experimentally examined the airflow within a corrugated channel with sharp and rounded corrugations where the convective heat transfer performance characteristics have been analyzed. At Reynolds number2000–5000, the height of channel was 5 mm; the corrugation angle was 30° the flow characteristics have been studied. They revealed that the performance of rounded corrugation is 100% superior than the sharp corrugation of corrugated channel. The flow characteristics and heat transfer of air flow in corrugated channels under constant surface.

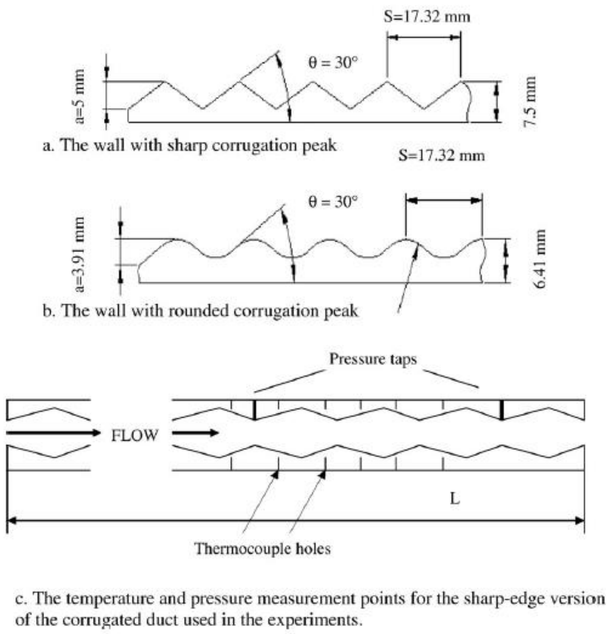

Figure 15 The converging–diverging channel with the representative parameters. [19]

Naphon et al. 2008 studied numerically and experimentally the heat transfer and fluid flow in the V-corrugated channel. The heat flux and Reynolds numbers were in the ranges of 0.5–1.2 kW/m2 and 400– 1600 respectively. The convection terms of governing equations were considered by upwind scheme and the SIMPLEC algorithm was used for coupling the velocity and pressure. The numerical simulation was implemented using commercial software NASTRAN/CFD. Results showed that the numerical simulation has agreed with the experimental measurement. It was found that the corrugated channel had significant influence on the heat transfer augmentation and the pressure drop penalty.

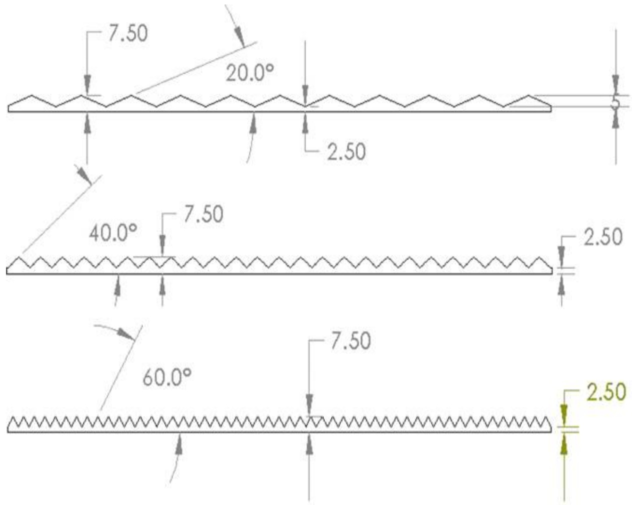

Figure 16 Schematic diagram of the corrugated plate. [20]

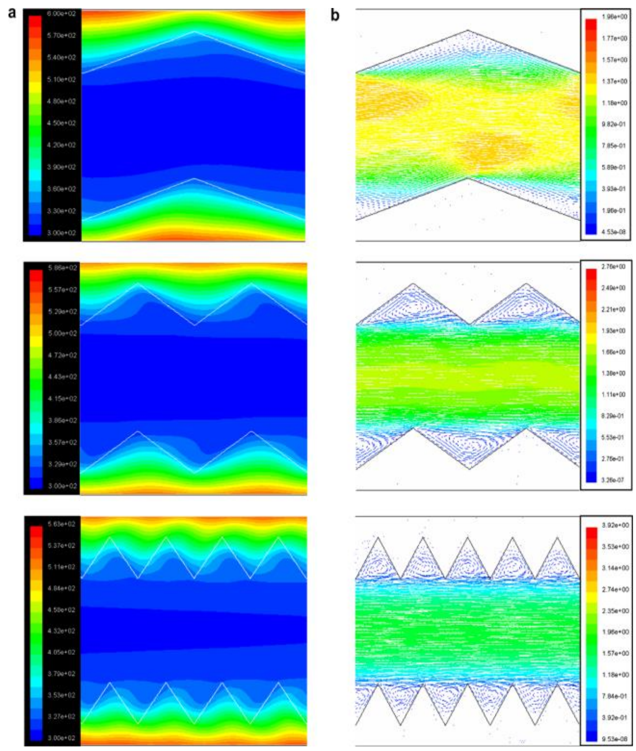

Figure 17 Variation of (a) temperature contour, (b) velocity vector for different channel heights at the same Re (918), wavy angle = 40^0, q = 0.83 kW/m² [21]

Metwally and Manglik 2004 performed numerically on the laminar convection in a sinusoidal corrugated channel with a constant temperature walls. The governing equations for mass, momentum, and energy have been solved by the finite difference approach over a nonorthogonal grid. The results indicated that the transverse vortices became more severe as the aspect ratio increased with a particular Reynolds number. Likewise, the mixing fluid was produced with the vortices enhancing significantly the rate of heat transfer that was dependent on the channel corrugation aspect ratios, Reynolds number, and Prandtl number. It was noticed that the area goodness factor for the sinusoidal channel was up to 5.5 times of the straight channel.

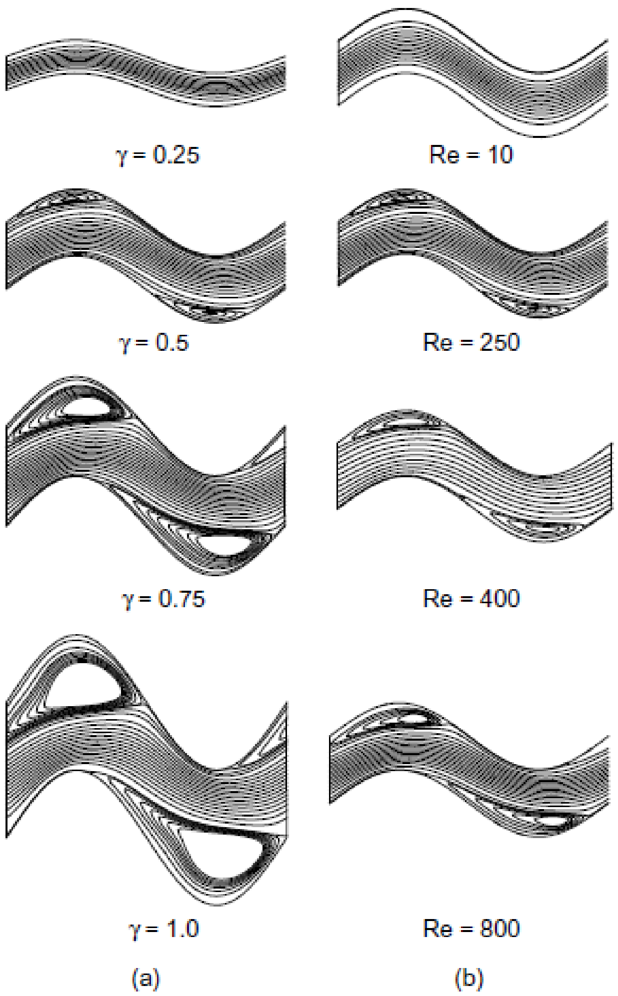

Figure 18 Streamline distributions in steady laminar flows in sinusoidal corrugated-plate channels [22]

Rush et al. 1999 experimentally performed the heat transfer and flow characteristics under sinusoidal wavy laminar flows through channel. Water tunnel was used to study the flow field using visualization methods while wind tunnel has been used to conduct heat transfer experiments in the range of Reynolds number 100 to 1000. It was observed that the geometry of the channel and Reynolds number have affected directly the location of the mixing onset. The heat transfer has been significantly increased by the onset of macroscopic mixing.

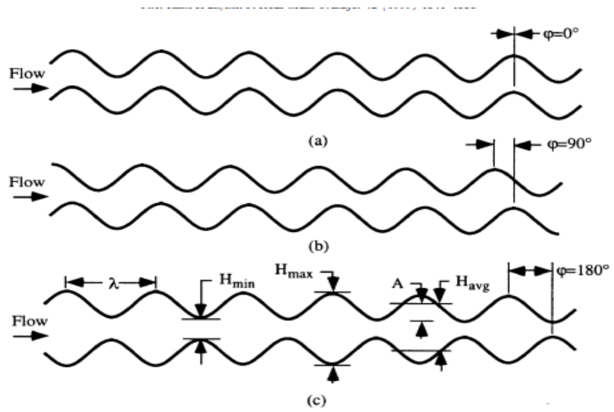

Figure 19 Schematic of wavy passage configurations and the definition of important geometric parameters "depth of channel is L"

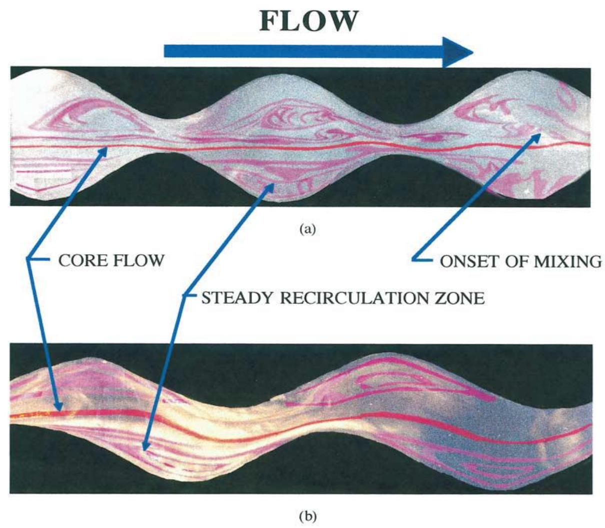

Figure 20 Typical images from the flow visualization study [22]

Wang and Chen 2002 investigated theoretically the heat transfer through a sinusoidal-wavy channel under the range of Reynolds number 100 to 700. The governing equations have converted the Cartesian coordinate to curvilinear coordinate by employing a simple coordinating transformation. Additionally, there was a slight heat transfer augmentation at smaller value of amplitude-wavelength ratio, while at larger value of amplitude-wavelength ratio. A significant enhancement in the heat transfer for higher Reynolds numbers was observed.

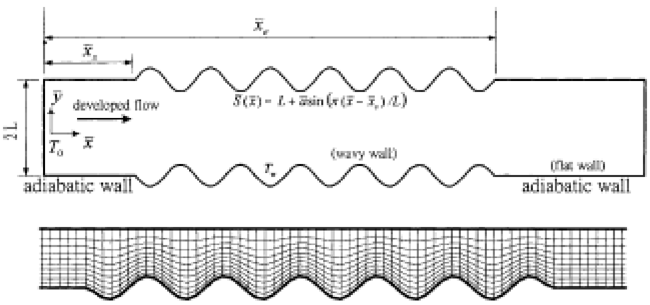

Figure 21 Physical model, coordinates and grid system [23]

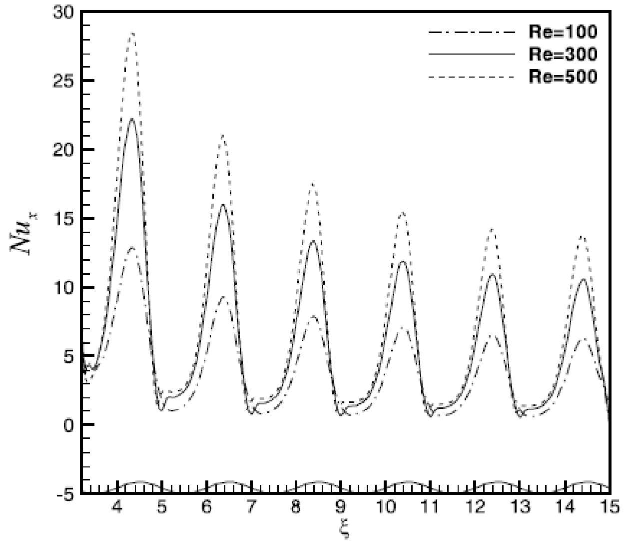

Figure 22 Distribution of local Nusselt number for a = 0:2 and Pr= 6:93. [24]

6. CONCLUSIONS

- Discrete, wavy and corrugated fins certainly yield higher transfer performance regardless of fin pattern, fin spacing, fin thickness and number of tubes compared to flat plate fins. However, at very low fin spacing and Re number, this superiority might get lost.
- Louver fins provide higher heat transfer rate as compared to plain fins, offset-strip fins and slit fins at same Re number. While for large number of tube rows slit fins are beneficial compared to louver fins. Convex louver fins are highly effective than louver and plane fins in terms of heat transfer rate and pressure loss. As they are capable of intensifying turbulent intensity of fluid flow.
- It has been reported that influence of fin spacing is monotonic and obscured on heat transfer and friction characteristics. Only at higher Reynolds number (Re>1000), Fp has no effect on j and f factor and at lower Reynolds number (Re < 1000) j factor decreases with the reduction of fin spacing.
- Staggered alignment as compared to inline alignment of tubes in CHXs leads to the higher heat transfer performance at the expense of larger pressure drop.
- It was reported by many investigators that number of tube rows has negligible impact on friction factor (f).
- Elliptical tubes provide lesser drag as compared to circular tubes which is the main reason that oval tubes yield better heat transfer characteristics.
- Position of tubes in downstream region instead of upstream region is preferred as higher heat transfer enhancement appears due to the significant horseshoe vortex formation.

REFERENCES

[1] A.A. Bhuiyan, A.S. Islam, CFD analysis of different fin-and-tube heat exchangers, J. Mech. Eng. 62 (4) (2011) 237–249.

[2] T.L. Bergman, F.P. Incropera, Fundamentals of Heat and Mass Transfer, John Wiley & Sons, 2011.

[3] K. Thulukkanam, Heat Exchanger Design Handbook, CRC Press, 2013.

[4] Q. Li et al., Compact heat exchangers: a review and future applications for a new generation of high temperature solar receivers, Renew. Sustain. Energy Rev. 15 (9) (2011) 4855–4875.

[5] F. Frass, R. Hofmann, K. Ponweiser, Principles of Finned-Tube Heat Exchanger Design for Enhanced Heat Transfer, Inst. f. Thermodynamics and Energy Conversion, Vienna University of Technology, 2007.

[6] C.-C. Wang, Investigation of wavy fin-and-tube heat exchangers: a contribution to databank, Exp. Heat Transfer 12 (1) (1999) 73–89.

[7] Arun Kumar Tiwari Pradyumna Ghosh and Jahar Sarkar, "Heat transfer and pressure drop characteristics of CeO2/water nanofluid in plate heat exchanger", Applied Thermal Engineering Volume 57, Issues 1–2, August 2013, Pages 24-32

[8] A.E.Kabeela, T.Abou El Maaty, and Y.El Samadony, "The effect of using nano-particles on corrugated plate heat exchanger performance", Applied Thermal Engineering, Volume 52, Issue 1, 5 April 2013, Pages 221-229

[9] C. Wang, P. Chen, J. Jang, Heat transfer and friction characteristics of convex louver fin-and-tube heat exchangers, Exp. Heat Transfer 9 (1) (1996) 61–78

[10] N.-H. Kim, An experimental investigation on the air-side performance of fin-and-tube heat exchangers having radial slit fins, Int. J. Air-Cond. Refrig. 23 (03) (2015) 1550021.

[11] F.S. Javadi, S. Sadeghipour, R. Saidur, G. BoroumandJazi, B. Rahmati, M.M. Elias, M.R. Sohel, "The effects of nanofluid on thermo-physical properties and heat transfer characteristics of a plate heat exchanger", International Communications in Heat and Mass Transfer, Volume 44, 2013, pp. 58-63

[12] Timo Laukkanen, Ari Seppälä, "Interplant heat exchanger network synthesis using nanofluids for interplant heat exchange", Applied Thermal Engineering, Volume 135, 5 May 2018, Pages 133-144

[13] Junyub Lim, Kang Sub Song, Dongwoo Kim, DongChan Lee, Yongchan Kim, "Condensation heat transfer characteristics of R245fa in a shell and plate heat exchanger for high-temperature heat pumps", International Journal of Heat and Mass Transfer, Volume 127, Part A, December 2018, Pages 730-739

[14] Kafel A. Mohammed, A.R. Abu Talib, A.A. Nuraini, K.A. Ahmed, Review of forced convection nanofluids through corrugated facing step, Renewable and Sustainable

Energy Reviews, Volume 75, August 2017, Pages 234-241

[15] S. Laohalertdecha, S. Wongwises, The effects of corrugation pitch on the condensation heat transfer coefficient and pressure drop of R-134 inside horizontal corrugated tube, Int. Comm. Heat Mass Transfer 53 (2010) 2924–2931.

[16] K. Aroonrat, A.S. Dalkilic, S. Wongwises, P. Promvonge. "Experimental study on evaporative heat transfer and pressure drop of R-134a flowing downward through vertical corrugated tubes with different corrugation pitches", Experimental Heat Transfer 26(2013) 41–63.

[17] Zhenping Wan, Qinghong Lin, Xiaowu Wang, Yong Tang, Flow characteristics and heat transfer performance of half-corrugated microchannels, Applied Thermal Engineering, Volume 123, August 2017, Pages 1140-1151

[18] Zhang L, Che D. Influence of corrugation profile on the thermal-hydraulic performance of cross-corrugated plates. Numer Heat Transf A: Appl 2011;59(4):267–96.

[19] Islamoglu Y. Effect of rounding of protruding edge on convection heat transfer in a converging-diverging channel. Int Commun Heat Mass Transf 2008;35(5):643–7.

[20] Naphon P. Effect of corrugated plates in an in-phase arrangement on the heat transfer and flow developments. Int J Heat Mass Transf 2008;51(15):3963–71

[21] Metwally HM, Manglik RM. Enhanced heat transfer due to curvature induced lateral vortices in laminar flows in sinusoidal corrugated-plate channels. Int J Heat Mass Transf 2004;47(10):2283–92.

[22] Rush TA, Newell TA, Jacobi AM. An experimental study of flow and heat transfer in sinusoidal wavy passages. Int J Heat Mass Transf 1999;42(9):1541–53

[23] Wang CC, Chen CK. Forced convection in a wavy-wall channel. Int J Heat Mass Transf 2002;45(12):2587–95.